

# Multispectral image pansharpening based on the contourlet transform

Israa Amro and Javier Mateos

**Abstract** Pansharpening is a technique that fuses the information of a low resolution multispectral image and a high resolution panchromatic image, usually remote sensing images, to provide a high resolution multispectral image. In the literature, this task has been addressed from different points of view being one of the most popular the wavelets based algorithms.

Recently, a new transform, the contourlet transform, has been proposed. This transform combines the advantages of the wavelets transform, with a more efficient directional information representation. The result is a flexible multiscale, multidirection and shift-invariant decomposition that can be efficiently implemented via the a'trous algorithm.

In this paper we compare the wavelet based pansharpening with existing contourlet based approaches and propose a new pansharpening method based on the contourlet transform. The performance of the contourlet in general, and the proposed method in particular, is assessed numerically and visually for Landsat and SPOT images.

## 1 Introduction

Earth observation satellites provide two different classes of images: a panchromatic image (PAN) with high spatial and low spectral resolutions and a multispectral image (MS) with high spectral and low spatial resolutions. In optical remote sensing, with physical and technological constraints, some satellite sensors supply the spectral bands needed to distinguish features spectrally but not spatially, while other

---

Israa Amro  
Universidad de Granada, Granada-Spain, e-mail: iamro@correo.ugr.es  
Al-Quds Open University, Hebron-Palestine, e-mail: isamro@qou.edu

Javier Mateos  
Universidad de Granada, Granada-Spain, e-mail: jmd@decsai.ugr.es

satellite sensors supply the spatial resolution for distinguishing features spatially but not spectrally. The fusion of high spatial resolution PAN image and the high spectral resolution MS image, providing more comprehensive information [1], is an important issue for many remote sensing and mapping applications. In general, pansharpening algorithms improve the spatial resolution of the MS image while simultaneously retaining its spectral information [2] and provides feature enhancement and improved classification as information from two different images is used effectively [3]. Nowadays pansharpened products are becoming very popular (see, for example, Google Earth [4]) and data providers are offering higher and higher amounts of them at lower and lower costs [5].

In the literature many pansharpening methods have been proposed for combining PAN with MS image, see [3, 5] for a detailed review. Among them, methods such as Intensity-Hue-Saturation (IHS) [6] and Principal Component Substitution (PCS) [7, 8] provide superior visual high-resolution multispectral images but ignore the requirement of high-quality synthesis of spectral information. More recently, an underlying multi-resolution analysis employing the discrete wavelet transform has been used in image fusion. It was found that multi-sensor image fusion is a trade-off between the spectral information from an MS sensor and the spatial information from an PAN sensor. With the wavelet transform fusion methods, it is easy to control this trade-off. Properties, such as multiresolution, localization, critical sampling, and limited directionality (horizontal, vertical, and diagonal directions) have made the wavelet transform a popular choice for feature extraction, image denoising, and pansharpening. However, wavelets fail to capture the smoothness along the contours [9]. The contourlet transform, an alternative multiresolution approach, provides an efficient directional representation and also efficient in capturing intrinsic geometrical structures of the natural image along the smooth contours [10]. Remote sensing images have presence of natural and man-made objects, e.g., rivers, roads, coastal areas, buildings, etc. which indicate higher geometrical content. Thus, the transformations taking in consideration the geometric structure along with other properties of wavelet transformation will be more useful for pansharpening.

In most of the proposed methods no explicit physical information about the detection system has been taken into account. However, a new technique proposed in [11] was used to define a wavelet-based fusion method which does incorporate information from the spectral response of the sensor in each band of the low-resolution MS image (LRMS). This prior knowledge is employed in the transformation model which injects spatial detail into the LRMS image. In this paper we will briefly describe the wavelet based pansharpening algorithms and the contourlet based algorithms sharing the same ideas, propose a new method that cast the WiSpeR method defined in [11] using the contourlet transform and we compare it with some of the most popular methods for pansharpening described in the literature.

The paper is organized as follows. Section 2 provides a short explanation of the contourlet transform. Section 3 describes the contourlet based pansharpening and the proposed algorithm. Experimental results and comparisons are presented in Section 4 for different datasets and, finally, Section 5 concludes the paper.

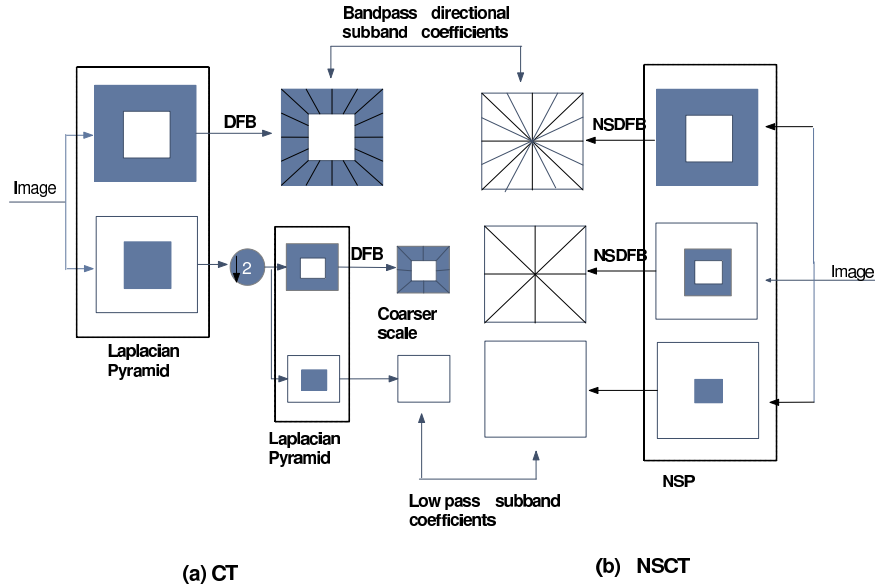


**Fig. 1** Discrete contourlet transform: a) Subsampled Contourlet Transform. b) Non-sampled Contourlet Transform

## 2 Contourlet transform

Contourlets provide a new system representation for image analysis [10]. The contourlet transform is so called because of its ability to capture and link the point of discontinuities to form a linear structure (contours). The two-stage process used to derive the contourlet coefficients involves a multiscale transform and a local directional transform. The point of discontinuities and multiscale transformation is obtained via the Laplacian pyramid. The local directional filter bank is used to group these wavelet-like coefficients to obtain a smooth contour. Contourlets provide  $2l$  directions at each scale, where  $l$  is the number of required orientation. This flexibility of having different numbers of direction at each scale makes contourlets different from other available multiscale and directional image representation [12]. Similarly to wavelets, contourlets also have different implementations of the subsampled and nonsubsamped transforms:

1. *Discrete Contourlet Transform (CT)*: The discrete CT is developed in the discrete domain using the fast iterated nonseparable filter banks having an order of  $N$  operations for  $N$ -pixel images. The transformation stage includes two filter banks: the Laplacian pyramid to generate multiscale decomposition and the directional filter bank (DFB) to reveal directional details at each decomposition level [10] as illustrated in Fig. 1(a). Similarly to the discrete wavelet transform, the discrete contourlet transform is also shift variant.

2. *Nonsubsampled Contourlet Transform (NSCT)*: The NSCT provides a complete shift-invariant and multiscale representation, similar to the redundant wavelet transform [13], with a fast implementation. The building block of the NSCT is the 2-D two-channel nonsubsampled filter banks (NSFBs). The NSCT is also obtained via a two stage non shift-invariant process [13] as depicted in Fig. 1(b). The first part achieves the multiscale property, via the nonsubsampled pyramid (NSP) subband decomposition, while the second part provides directionality information using nonsubsampled directional filter bank (NSDFB). Both stages of the NSCT are constructed to be invertible in order to have an overall invertible system.

### 3 Wavelet and Contourlet-based pansharpening

A number of pansharpening methods using the wavelet and, more recently, the contourlet transform has been proposed. In general, all the transform based fusion methods consist of three stages. The first stage provides a sub-band and directional decomposition by the application of the subsampled or non-subsampled wavelet or contourlet transform to the PAN and MS images. It is followed by the application of various fusion rules onto the transform coefficients. These fusion rules usually comprise, for instance, substituting the original MS coefficient bands by the coefficients of the PAN image or adding the coefficients of the PAN to the coefficients of the original MS bands weighted sometimes, like for the method we propose in this paper, by a factor related with the contribution of the PAN image to each MS band. The fusion schemes ends with the inverse transform.

This paper summarizes the most important wavelet-based pansharpening methods, and compares them with the existing contourlet-based ones and the new proposed contourlet method. Since contourlet-based and wavelet-based methods share same stages for similar methods, except the transform type (contourlet or wavelet), let us to describe them together.

#### 3.1 Additive Wavelet/Contourlet

The steps for fusing MS and PAN images using the additive wavelet [14] /contourlet [15] method are:

1. Register the LRMS image to the same size as the PAN image in order to be superimposed.
2. For each band of the MS image taken into account, generate a new panchromatic image which histogram match that of the MS image using, for instance, [16]

$$PAN_k = (PAN - \mu_{PAN}) \frac{\sigma_{b_k}}{\sigma_{PAN}} + \mu_{b_k}, \quad (1)$$

where  $\mu_{PAN}$ ,  $\mu_{b_k}$  are the mean of the PAN and the MS band  $b_k$ , respectively,  $k \in B$ , and  $B$  is the set of bands we are interested in.  $\sigma_{PAN}$  and  $\sigma_{b_k}$  are the standard deviation of PAN and MS band  $b_k$ , respectively.

3. Apply the wavelet/contourlet transform to each histogram-matched panchromatic images. Repeat the same transform to each MS band.

$$PAN_k = \bigcup_{i=1}^n wPAN_k^i \cup PAN_k^r, \quad (2)$$

$$b_k = \bigcup_{i=1}^n wb_k^i \cup b_k^r, \quad \forall k \in B \quad (3)$$

where  $wPAN_k^i$  and  $wb_k^i$  are the wavelet/contourlet coefficients for PAN and MS bands, respectively,  $PAN_k^r$  and  $b_k^r$  are the residual (low pass filtered version of original) images of PAN and MS bands, respectively,  $n$  is the wavelet/contourlet resolution levels, usually  $n = 2$  or  $3$ . The  $\cup$  operator means the composition operator that merges the different wavelet/contourlet bands since each band may have different resolution. Note that in the non subsampled case, this operator means just adding the different bands.

4. Introduce the details of the panchromatic image into each MS band adding the wavelet/contourlet coefficients of the panchromatic image to those of the MS image

$$b_k^{coef} = \bigcup_{i=1}^n (wPAN_k^i + wb_k^i), \quad (4)$$

where  $b_k^{coef}$  is the new wavelet/contourlet coefficients of the MS band  $k$ .

5. Apply the inverse wavelet/contourlet transform to each MS transformed band

$$b_k^{new} = b_k^{coef} \cup b_k^r \quad (5)$$

to obtain  $b_k^{new}$ , the pansharpened MS band  $k$ ,  $k \in B$ . Note that since for the undecimated case,  $\sum_{i=1}^n wb_k^i + b_k^r = b_k$ , we don't need to decompose the MS image and we can add  $b_k$  to the corresponding PAN coefficients.

### 3.2 Substitutive wavelet/contourlet

The substitute wavelet/contourlet methods are quite similar to the additive ones but, instead of adding the information of the panchromatic image to each band of the MS image, the pansharpening method simply replaces the MS detail bands with the details obtained by the panchromatic image following these steps for wavelet [17] and contourlet [18] reconstruction:

1. Perform the first 3 steps of the algorithm described in section 3.1.

2. For each MS band  $k$ , perform the inverse wavelet/contourlet transform to the transformed image formed by the wavelet/contourlet coefficient planes of the histogram-matched PAN image  $wPAN_k^i, i = 1 \dots n$ , and the residual band of the MS image  $k$ , that is,

$$b_k^{new} = \bigcup_{i=1}^n wPAN_k^i \cup b_k^r. \quad (6)$$

### 3.3 IHS wavelet/contourlet

One of the most popular image pansharpening methods are those based on the IHS transformation. The main drawback of these methods is the high distortion of the original spectral information that the resulting MS images present. To avoid this problem, the IHS transformation is followed by the wavelet or contourlet transform to take advantage of the multiresolution property of this transform. Another disadvantage of the IHS based method, that cannot be solved by these transforms, is that they can only work with three bands due to the IHS transformation.

#### 3.3.1 Additive IHS

In order to perform the wavelet [14] and contourlet [19, 20] additive IHS pansharpening, the following steps are followed:

1. Register the LRMS image to the same size as the PAN image in order to be superimposed.
2. Apply the IHS transform to the RGB composition of three MS image, using,

$$\begin{pmatrix} I \\ v1 \\ v2 \end{pmatrix} = \begin{pmatrix} \frac{1}{3} & \frac{1}{3} & \frac{1}{3} \\ \frac{-1}{\sqrt{6}} & \frac{-1}{\sqrt{6}} & \frac{2}{\sqrt{6}} \\ \frac{1}{\sqrt{6}} & \frac{-1}{\sqrt{6}} & 0 \end{pmatrix} \begin{pmatrix} R \\ G \\ B \end{pmatrix}, \quad (7)$$

$$H = \tan^{-1} [v2/v1], S = \sqrt{v1^2 + v2^2}.$$

3. Perform histogram matching between the panchromatic image and the intensity component of the IHS image using Eq. (1) to obtain  $PAN_I$ , the PAN image histogram-matched to the  $I$  band.
4. Apply wavelet/contourlet decomposition algorithm to the  $I$  band of the IHS image and to the histogram-matched PAN one using,

$$I = \bigcup_{i=1}^n wI^i \cup I^r, \quad (8)$$

$$PAN_I = \bigcup_{i=1}^n wPAN_I^i \cup PAN_I^r. \quad (9)$$

5. Generate the wavelet/contourlets coefficients of the pansharpened intensity image as the sum of the wavelet/contourlet coefficients of the initial intensity and the histogram-matched PAN image,

$$I^{coef} = \bigcup_{i=1}^n (wPAN_I^i + wI^i). \quad (10)$$

6. Apply the inverse wavelet/contourlet transform to reconstruct new intensity image  $I^{new}$ ,

$$I^{new} = I^{coef} \cup I^r. \quad (11)$$

Note that, as already happened in the additive wavelet case, since for the undecimated case  $\sum_{i=1}^n wI^i + I^r = I$ , we don't need to decompose the  $I$  image.

7. Insert the spatial information of the panchromatic image into the MS one, by applying the inverse IHS transform,

$$\begin{pmatrix} R^{new} \\ G^{new} \\ B^{new} \end{pmatrix} = \begin{pmatrix} 1 & \frac{-1}{\sqrt{6}} & \frac{3}{\sqrt{6}} \\ 1 & \frac{-1}{\sqrt{6}} & \frac{-3}{\sqrt{6}} \\ 1 & \frac{2}{\sqrt{6}} & 0 \end{pmatrix} \begin{pmatrix} I^{new} \\ v1 \\ v2 \end{pmatrix}. \quad (12)$$

### 3.3.2 Substitutive IHS

In order to perform the wavelet [21] and contourlet substitutive IHS pansharpening, the following steps are followed:

1. Perform the first 4 steps of the section 3.3.1.
2. Perform the inverse wavelet/contourlet transform to the wavelet/contourlet image formed by substituting the wavelet/contourlet coefficient planes of the intensity image with the corresponding wavelet/contourlet planes of the histogram-matched PAN image,

$$I^{new} = \bigcup_{i=1}^n wPAN_I^i \cup I^r. \quad (13)$$

3. Apply the inverse IHS transform using Eq. (12).

### 3.4 PCA wavelet/contourlet

The PCA-based method has been popularly used for spectral transformation because the first principal component (PC1) consists of the most variance, making it a suitable choice to replace the PAN component. Like IHS, the main drawback of this

method is the high distortion of the original spectral information that the resulting MS images may present. To overcome this problem, Gonzalez et al. [22] proposed a pansharpening method based the PCA and wavelets methods where only the details of PC1 are replaced by the details of the PAN image.

The steps we need to pansharpen an image using the PCA wavelet [14] and contourlet [12] methods are the following:

1. Register the LRMS image to the same size as the PAN image in order to be superimposed.
2. Apply the PCA transformation to the MS image to obtain the PC1 image.
3. Histogram match the PAN image to the PC1 image.
4. Apply a subsampled or non-subsampled wavelet or contourlet transformation to the PC1 image and the histogram matched PAN image.
5. Replace the detail wavelet or contourlet coefficients of PC1 with the detail wavelet or contourlet coefficients of the histogram-matched PAN image.
6. Perform inverse wavelet/contourlet transformation and inverse PCA transformation to obtain a PAN image.

### 3.5 *WiSpeR/ CiSpeR*

The WiSpeR method can be understood as a generalization of different wavelet-based image fusion methods [11]. It uses a modification of the non-subsampled additive wavelet algorithm where the contribution from the PAN image to each of fused bands depends on a factor generated both from the sensor spectral response and physical properties of the observed object.

The steps for merging MS and PAN images using WiSpeR method are as follows:

1. Register the LRMS image to the same size as the PAN image in order to be superimposed.
2. Generate new panchromatic images, whose histograms match those of each band of the MS image, using Eq. (1).
3. Perform the  $n$  undecimated wavelet planes transform only on the panchromatic images, using Eq. (2).
4. Calculate the spectral factor  $\lambda_k$ , related to  $b_k$  bands [11], where  $k$  is the band number.
5. Add the wavelet planes of the panchromatic decomposition to each band of the MS dataset, as the following:

$$b_k^{new} = b_k + \lambda_k \sum_{i=1}^n wPAN_k^i, \quad (14)$$

where  $b_k^{new}$  is the fused band  $k$ ,  $k \in B$ , and  $B$  is the number of bands we take into account.



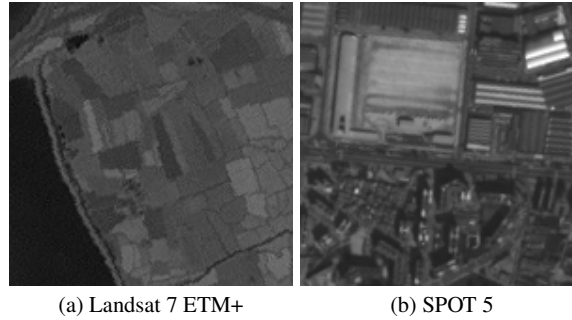


**Fig. 2** Panchromatic Imagery of the Dataset

We proposed a new contourlet panshaping method, named CiSpeR, that, similarly to WiSpeR, depends on a spectral factor to determine the amount of spatial detail of the PAN image that has to be injected into each MS band but it uses the non-subsampling contourlet transform with necessary filters, and  $n$  resolution levels and  $m$  directions in each level.

## 4 Experimental Results

The contourlet-based and wavelet-based methods mentioned in section 3 are evaluated by performing pansharpening on dataset acquired by SPOT5, and Landsat 7 ETM+ satellites. The MS and PAN images are co-registered for each dataset. The panchromatic images, for both SPOT5 and Landsat 7 ETM+, are shown in Fig. 2.

In the Landsat 7 ETM+ Dataset, we chose a region of interest of the MS image of 256 by 256 pixels with a pixel resolution of 28.5 m, and a region of interest of the PAN image of 512 by 512 pixels, with a pixel resolution of 14.25 m. The MS image consists of six bands from the visible and infrared (IR) region as follows: blue (0.45-0.515  $\mu\text{m}$ ), green (0.525-0.605  $\mu\text{m}$ ), red (0.63-0.690  $\mu\text{m}$ ), Near IR (0.75-0.90  $\mu\text{m}$ ), Mid IR (1.55-1.75  $\mu\text{m}$ ), and Mid IR (2.09-2.35  $\mu\text{m}$ ). The PAN image consists of a single band covering the visible and Near IR (0.52-0.90  $\mu\text{m}$ ). The scene, depicted in Fig. 3(a), was acquired over The Netherlands on May 13, 2000.

The MS image in SPOT5 dataset covers a region of interest of 256 by 256 pixels with a pixel resolution of 10 m, while the PAN image is 512 by 512 pixels with a pixel resolution of 5 m. The MS image consists of four bands from the visible and infrared region corresponding to green (0.50-0.59  $\mu\text{m}$ ), red (0.61-0.68  $\mu\text{m}$ ), Near IR (0.78-0.89  $\mu\text{m}$ ), Mid IR(1.58-1.75  $\mu\text{m}$ ), while the PAN image consists of a single band covering the visible and NIR (0.48-0.71  $\mu\text{m}$ ). The scene, depicted in Fig. 4(a), was acquired over Sevilla (Spain) on February 15, 2003.

Pansharpening results are evaluated visually and numerically using some well known global quality indexes. The Correlation coefficient (COR) [23] is a normalized index that takes values between 0 and 1 (the higher the value the better the

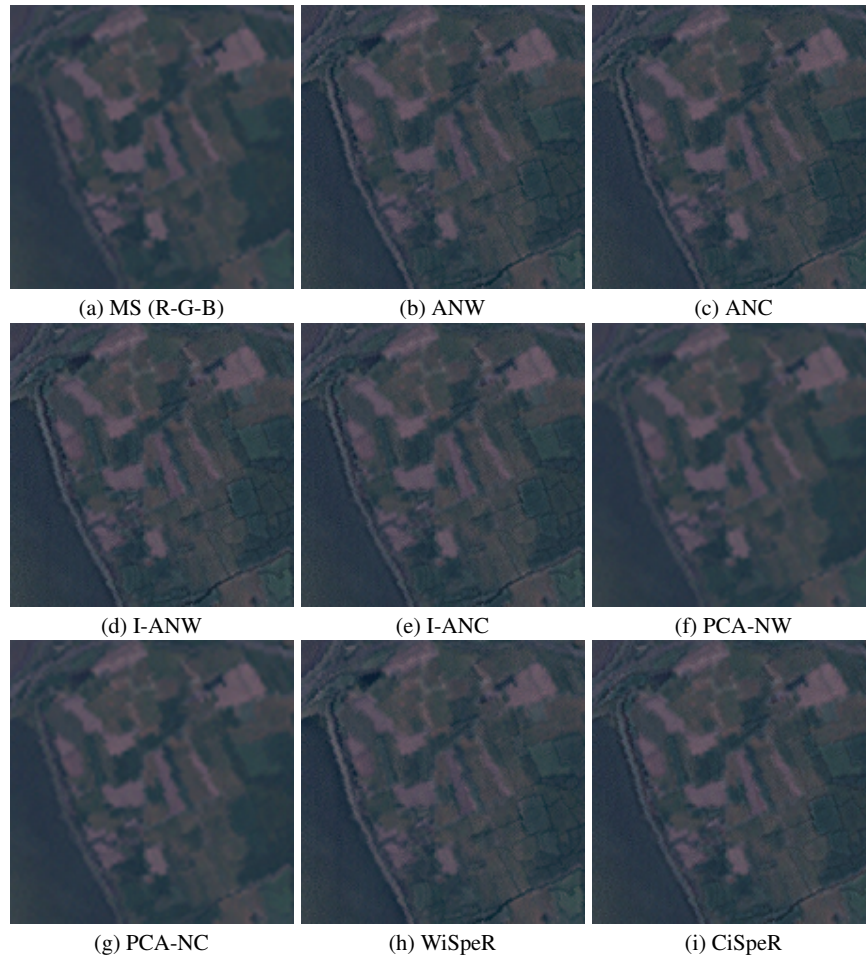


**Fig. 3** (a) Low resolution image formed from the R-G-B bands of the MS LandSat image. (b)–(i) Pansharpened images using the methods under study.

quality of the reconstruction) that assess the spatial similarity between each reconstructed multispectral image band and the panchromatic image. Spectral fidelity is assessed by means of the Universal Image Quality Index (UIQI) [24], which also takes values between 0 and 1, indicating a value of 1 the best quality, and the *erreur relative globale adimensionnelle de synthèse* (ERGAS) [25] index, whose English translation is relative dimensionless global error in fusion, a global criterion for what the lower the value, the higher the quality of the multispectral image.

Since more than twenty methods for pansharpening have been presented, due to lack of space we compare in this paper the pansharpening methods from the discussed above that, from our point of view, are the most significant. In our preliminary experiments we have realized that the non-subsampled decompositions al-

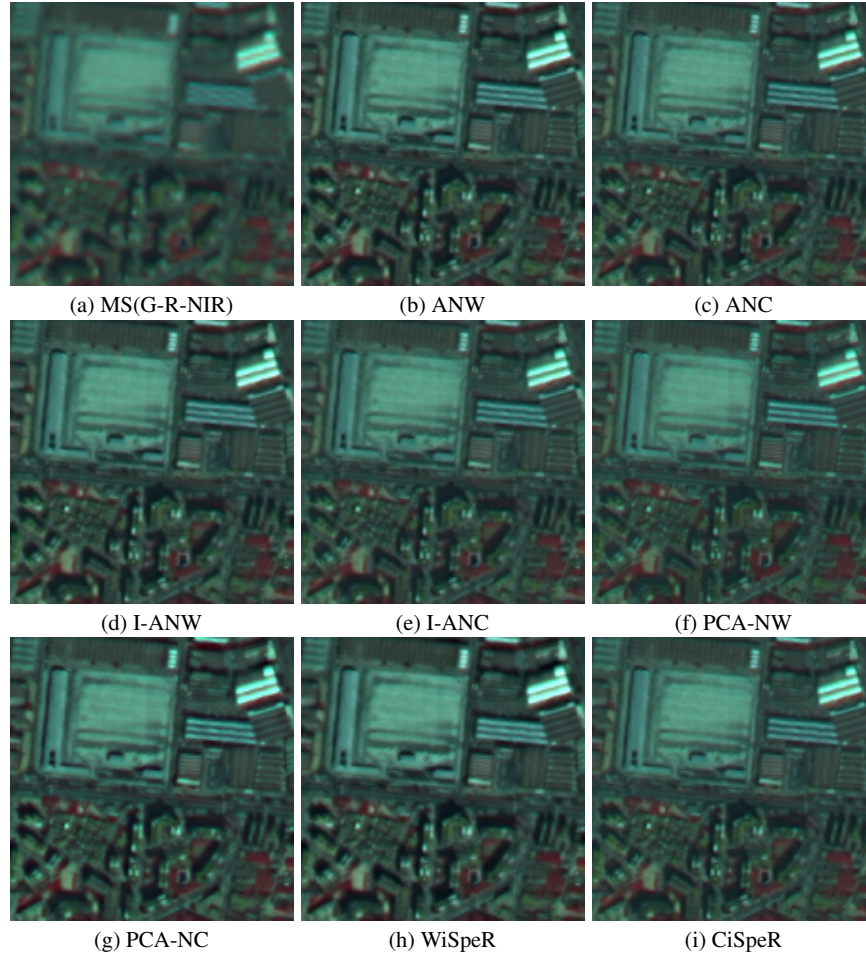


**Fig. 4** (a) Low resolution image formed from the G-R-NIR bands of the MS SPOT image. (b)–(i) Pansharpened images using the methods under study.

ways provide better results than their subsampled counterpart so we are going to center on the non-subsampled approaches. Also, we realized that, usually, the additive methods performs better than the substitute ones so, in this paper, we are going to compare the following eight methods: Additive Non-subsampled Wavelet (ANW), IHS Additive Non-subsampled Wavelet (I-ANW), PCA Non-subsampled Wavelet (PCA-NW), Additive Non-subsampled Contourlet (ANC), IHS Additive Non-subsampled Contourlet (I-ANC), PCA Non-subsampled Contourlet (PCA-NC), WiSpeR, and CiSpeR.

The pansharpened images resulted from using the wavelet/contourlet methods under study are presented in Fig. 3 for Landsat 7 dataset, and in Fig. 4 for SPOT 5 dataset. From the pansharpened images we observe that the contourlet-based and

Measure	Band	ANW	ANC	I-ANW	I-ANC	PCA-NW	PCA-NC	WiSpeR	CiSpeR
<b>COR</b>	b1	0.81	0.86	<b>0.87</b>	<b>0.90</b>	0.33	0.33	<b>0.87</b>	<b>0.90</b>
Ideal Value =1	b2	0.85	0.88	0.89	<b>0.91</b>	0.48	0.47	0.88	<b>0.90</b>
	b3	<b>0.90</b>	<b>0.90</b>	0.84	<b>0.85</b>	0.41	0.40	0.79	0.80
	b4	<b>0.95</b>	<b>0.95</b>	-	-	<b>0.93</b>	0.91	0.84	0.85
<b>UIQI</b>	b1	0.77	0.84	0.70	0.79	<b>0.94</b>	<b>0.95</b>	0.57	0.79
Ideal Value =1	b2	0.81	0.87	0.76	0.83	<b>0.95</b>	<b>0.96</b>	0.66	0.85
	b3	0.80	0.87	0.88	0.91	<b>0.96</b>	<b>0.97</b>	0.89	0.93
	b4	0.83	0.86	-	-	0.77	<b>0.88</b>	<b>0.88</b>	<b>0.93</b>
<b>ERGAS</b>	-	5.08	3.51	4.25	2.77	3.25	<b>2.08</b>	4.72	<b>2.50</b>
Ideal = Lowest	-	-	-	-	-	-	-	-	-

**Table 1** Landsat 7 ETM+ Quantative Analysis

the new pansharpening method not only enhance the spatial resolution, but also preserve the spectral information of the original MS image better than wavelet ones. Although the IHS-based fusion methods improve the spatial resolution, they induce some color distortion, so these methods cannot be used to preserve the spectral information effectively. The additive contourlet method preserves the spectral information to some extent; however it contains less spatial information which is manifested as blur on the fused image. PCA-based resulted image with Landsat does not differ of the original MS image, while with SPOT dataset it improves the spatial resolution and preserves the spectral information of the original MS image. The proposed method, CiSpeR, enhances the images spatially while accurately preserves the spectral information for both imagery datasets..

The visual inspection of the images of Fig. 3 and Fig. 4 agree also with the quantitative analysis results. Table 1 shows the quantitative results for Landsat 7 imagery. The highlighted values in the table present the two highest ideal values for each measure. It is clear that the contourlet-based methods, have better results than wavelet ones except for the PCA based approaches where the non-subsampled wavelet-based method obtain slighter better values for the COR coefficient. These results are expected since the contourlet is known to have a better representation for directional information, and the nonsubsamped version provides a shift-invariant representation. The figures of merit in this table also indicate that some approaches, like PCA, are spectrally efficient but they did not add many spatial details, while the proposed CiSpeR approach achieves consistent results, spectrally and spatially, providing one of the highest COR values with one of the highest UIQI values and a very low ERGAS value.

Table 2 shows the evaluation results with the same quality indexes for SPOT 5 imagery. SPOT 5 quantative analysis again shows that contourlet-based methods provide better results compared to all other wavelet-based methods. Here all the contourlet-based methods performs very well, obtaining a high COR and high UIQI with low ERGAS, probably due to the high resolution of the images, with only 5 meter per pixel, that allows a very good representation of the spatial structures using the contourlet transform. For the SPOT image we can see that PCA give better results than PCA with Landsat. This may be due to the correlation between PC1 and

Measure	Band	ANW	ANC	I-ANW	I-ANC	PCA-NW	PCA-NC	WiSpeR	CiSpeR
<b>COR</b>	b1	0.90	0.92	<b>0.93</b>	<b>0.94</b>	0.83	0.85	0.90	0.92
Ideal Value =1	b2	0.95	<b>0.96</b>	0.91	0.93	<b>0.98</b>	0.95	0.92	0.94
	b3	0.94	<b>0.95</b>	0.93	<b>0.95</b>	<b>0.97</b>	<b>0.95</b>	0.93	<b>0.95</b>
	b4	0.93	<b>0.95</b>	-	-	<b>0.95</b>	<b>0.96</b>	0.88	0.92
<b>UIQI</b>	b1	0.86	0.91	0.83	0.88	<b>0.95</b>	<b>0.95</b>	0.79	<b>0.92</b>
Ideal Value =1	b2	0.91	0.94	<b>0.95</b>	<b>0.97</b>	0.93	<b>0.95</b>	0.89	<b>0.97</b>
	b3	0.91	<b>0.95</b>	0.92	<b>0.95</b>	0.93	<b>0.95</b>	0.85	<b>0.96</b>
	b4	0.82	0.88	-	-	0.88	<b>0.89</b>	0.85	<b>0.94</b>
<b>ERGAS</b>	-	5.36	3.52	5.40	3.30	3.25	<b>3.03</b>	5.27	<b>2.86</b>
Ideal = Lowest	-	-	-	-	-	-	-	-	-

**Table 2** SPOT 5 Quantative Analysis

MS bands. While, for the Landsat 7 image, PC1 is very similar to band 4, in SPOT 5 it takes information from the four bands. Again, CiSpeR almost achieves the ideal values in all the spatial and spectral measures.

## 5 Conclusions

In this paper, wavelet and contourlet based pansharpening approaches have been compared and their efficiency to merge Landsat 7 and SPOT images has been evaluated by means of visual and quantative analysis.

Different image pansharpening methods based on the undecimated wavelet and contourlet transform (Additive, IHS and PCA) have been experimentally compared. Also the new proposed method CiSpeR was compared with these methods and with WiSpeR. In all methods, contourlet-based pansharpened images present, visually and numerically, better results than those obtained by wavelet for both Landsat and SPOT imagery extracting spatial information from the PAN image missing in the MS image, without modifying its spectral information content.

CiSpeR obtain a very low ERGAS value, smaller than 3, in both imagery, and values very close to the ideal in the other measures. It is a consistent approach that works well spatially and spectrally with different imagery dataset.

**Acknowledgements** This work has been supported by the Consejería de Innovación, Ciencia y Empresa of the Junta de Andalucía under contract P07-TIC-02698.

## References

1. Z. Wang, D. Ziou, C. Armenakis, D. Li, and Q. Li. A comparative analysis of image fusion methods. *IEEE Trans. Geosci. Remote Sens.*, 43(6):1391–1402, 2005.
2. L. Wald. Some terms of reference in data fusion. *IEEE Trans. Geosci. Remote Sens.*, 37(3):1190–1193, 1999.

3. C. Pohl and J. L. Van Genderen. Multi-sensor image fusion in remote sensing: Concepts, methods, and applications. *Int. J. Remote Sens.*, 19(5):823–854, 1998.
4. Google Earth, <http://earth.google.com/>. *Google Earth Web Site*.
5. L. Alparone, L. Wald, J. Chanussot, P. Gamba, and L. M. Bruce. Comparison of pansharpening algorithms: Outcome of the 2006 GRS-S data-fusion contest. *IEEE Trans. Geosci. Remote Sens.*, 45(10):3012–3021, 2007.
6. P. S. Chavez, Jr and J. A. Bowell. Comparison of the spectral information content of Landsat Thematic Mapper and SPOT for three different sites in the Phoenix, Arizona region. *Photogramm. Eng. Remote Sens.*, 54(12):1699–1708, 1988.
7. J. Zhou, D. L. Civco, and J. A. Silander. A wavelet transform method to merge Landsat TM and SPOT panchromatic data. *Int. J. Remote Sens.*, 19(4):743 – 757, 1998.
8. P. S. Chavez and A. Y. Kwarteng. Extracting spectral contrast in Landsat thematic mapper image data using selective principal component analysis. *Photogramm. Eng. Remote Sens.*, 55(3):339–348, 1989.
9. V. P. Shah, N. H. Younan, and R. King. Pan-sharpening via the contourlet transform. In *Proc. IEEE Int. Geosci. Remote Sens. Symp. IGARSS 2007*, pages 310–313, 23–28 2007.
10. M. N. Do and M. Vetterli. The contourlet transform: an efficient directional multiresolution image representation. *IEEE Trans. Image Process.*, 14(12):2091–2106, 2005.
11. X. Otazu, M. González-Audícana, O. Fors, and J. Núñez. Introduction of sensor spectral response into image fusion methods: Application to wavelet-based methods. *IEEE Trans. Geosci. Remote Sens.*, 43(10):2376–2385, 2005.
12. V. P. Shah, N. H. Younan, and R. L. King. An efficient pan-sharpening method via a combined adaptive PCA approach and contourlets. *IEEE Trans. Geosci. Remote Sens.*, 46(5):1323–1335, 2008.
13. A. L. da Cunha, Jianping Zhou, and M. N. Do. The nonsubsampling contourlet transform: Theory, design, and applications. *IEEE Trans. Image Process.*, 15(10):3089–3101, 2006.
14. M. González-Audícana and X. Otazu. Comparison between Mallat’s and the a’trous discrete wavelet transform based algorithms for the fusion of multispectral and panchromatic images. *Int. J. Remote Sens.*, 26(3):595–614, 2005.
15. M. Lillo-Saavedra and C. Gonzalo. Multispectral images fusion by a joint multidirectional and multiresolution representation. *Int. J. Remote Sens.*, 28(18):4065 – 4079, 2007.
16. W. Dou and Y. Chen. An improved IHS image fusion method with high spectral fidelity. *The Int. Archiv. of the Photogramm., Rem. Sensing and Spat. Inform. Sciences*, XXXVII:1253–1256, 2008. part.B7.
17. J. Núñez, X. Otazu, O. Fors, A. Prades, V. Pala, and R. Arbiol. Multiresolution-based image fusion with additive wavelet decomposition. *IEEE Trans. Geosci. Remote Sens.*, 37(3):1204–1211, 1999.
18. M. Song, X. Chen, and P. Guo. A fusion method for multispectral and panchromatic images based on HSI and contourlet transformation. In *Proc. 10th Workshop on Image Analysis for Multimedia Interactive Services WIAMIS ’09*, pages 77–80, 6–8 May 2009.
19. A. M. ALEjaily, I. A. El Rube, and M. A. Mangoud. Fusion of remote sensing images using contourlet transform. *Springer Science*, pages 213 – 218, 2008.
20. X.-H. Yang and L.-C. Jiao. Fusion algorithm for remote sensing images based on nonsubsampling contourlet transform. *Acta Automatica Sinica*, 34(2):274–281, 2008.
21. J. Wu, H. Huang, J. Liu, and J. Tian. Remote sensing image data fusion based on ihs and local deviation of wavelet transformation. In *Proc. IEEE Int. Conf. on Robotics and Biomimetics ROBIO 2004*, pages 564 – 568, 2004.
22. M. González-Audícana, J.L. Saleta, R. García Catalán, and R. García. Fusion of multispectral and panchromatic images using improved IHS and PCA mergers based on wavelet decomposition. *IEEE Trans. Geosc. Remote Sens.*, 42(6):1291–1298, 2004.
23. V. Vijayaraj, C. G. O’Hara, and N. H. Younan. Quality analysis of pansharpened images. In *Proc. IEEE Int. Geosc. Remote Sens. Symp. IGARSS ’04*, volume 1, 20–24 2004.
24. Z. Wang and A. C. Bovik. A universal image quality index. *IEEE Signal Process. Lett.*, 9(3):81–84, 2002.
25. L. Wald. Quality of high resolution synthesized images: Is there a simple criterion? *Proc. Int. Conf. Fusion of Earth Data. Nice, France*, 1:99 –105, 2000.